



# The Host Immune System Facilitates Disseminated *Staphylococcus aureus* Disease Due to Phagocytic Attraction to *Candida albicans* during Coinfection: a Case of Bait and Switch

Devon L. Allison,<sup>a</sup> Nina Scheres,<sup>b</sup> Hubertine M. E. Willems,<sup>c</sup> Carolien S. Bode,<sup>b</sup> Bastiaan P. Krom,<sup>b</sup> Mark E. Shirtliff<sup>a†</sup>

<sup>a</sup>Department of Microbial Pathogenesis, School of Dentistry, University of Maryland—Baltimore, Baltimore, Maryland, USA

<sup>b</sup>Department of Preventive Dentistry, Academic Centre for Dentistry Amsterdam (ACTA), Vrije Universiteit Amsterdam and the University of Amsterdam, Amsterdam, The Netherlands

<sup>c</sup>Department of Clinical Pharmacy, University of Tennessee Health Science Center, Memphis, Tennessee, USA

**ABSTRACT** Invasive *Staphylococcus aureus* infections account for 15 to 50% of fatal bloodstream infections annually. These disseminated infections often arise without a defined portal of entry into the host but cause high rates of mortality. The fungus *Candida albicans* and the Gram-positive bacterium *S. aureus* can form polymicrobial biofilms on epithelial tissue, facilitated by the *C. albicans* adhesin encoded by *ALS3*. While a bacterium-fungus interaction is required for systemic infection, the mechanism by which bacteria disseminate from the epithelium to internal organs is unclear. In this study, we show that highly immunogenic *C. albicans* hyphae attract phagocytic cells, which rapidly engulf adherent *S. aureus* and subsequently migrate to cervical lymph nodes. Following *S. aureus*-loaded phagocyte translocation from the mucosal surface, *S. aureus* produces systemic disease with accompanying morbidity and mortality. Our results suggest a novel role for the host in facilitating a bacterium-fungus infectious synergy, leading to disseminated staphylococcal disease.

**KEYWORDS** *Candida albicans*, *Staphylococcus aureus*, biofilms, innate immunity, polymicrobial

Within environmental systems and hosts, microorganisms exist in complex multi-species communities rather than as isolated organisms. The formation of polymicrobial biofilms, which protects numerous bacteria and fungi within a polysaccharide extracellular matrix (1, 2), involves complex interspecies and interkingdom interactions (3). The formation of biofilms on devitalized tissues, on medical devices, and within immunocompromised patients continues to burden health care communities worldwide; biofilm-mediated infections account for about 25% of all nosocomial infections (4, 5). The incidence of polymicrobial implant-associated infections underwent an alarming 5-fold increase in 6 years (from 2004 to 2010, a period during which clinical protocols for detection and treatment were improved), highlighting the importance of this etiology in clinical care (6).

The Gram-positive bacterium *Staphylococcus aureus* and the polymorphic fungus *Candida albicans* are biofilm-forming, opportunistic pathogens capable of colonizing multiple niches in humans (7–9). *S. aureus* has remained in the spotlight due to the burgeoning increase in methicillin-resistant *Staphylococcus aureus* (MRSA) strains and the narrowing spectrum of effective antibiotics (10). The Centers for Disease Control and Prevention (CDC) estimates that 33% of the population carry *S. aureus* in their nares, while 2% harbor MRSA (7). This bacterium possesses a wide range of virulence factors, including immunoavoidance mechanisms, toxins, antimicrobial resistance determinants, and adherence proteins, which allow for increased pathogenesis (11). The production of toxins by community-associated strains, which tend to infect healthy

**Citation** Allison DL, Scheres N, Willems HME, Bode CS, Krom BP, Shirtliff ME. 2019. The host immune system facilitates disseminated *Staphylococcus aureus* disease due to phagocytic attraction to *Candida albicans* during coinfection: a case of bait and switch. *Infect Immun* 87:e00137-19. <https://doi.org/10.1128/AI.00137-19>.

**Editor** Victor J. Torres, New York University School of Medicine

**Copyright** © 2019 American Society for Microbiology. All Rights Reserved.

Address correspondence to Devon L. Allison, [devon.allison@umaryland.edu](mailto:devon.allison@umaryland.edu).

† Deceased.

D.L.A. and N.S. contributed equally to this work. B.P.K. and M.E.S. contributed equally to this work.

**Received** 24 May 2019

**Returned for modification** 23 June 2019

**Accepted** 18 August 2019

**Accepted manuscript posted online** 26 August 2019

**Published** 18 October 2019

individuals, is predicted to be regulated by unique genetic mechanisms, which enable rapid dissemination *in vivo* and increase the risk of necrotizing pneumonia (12). Despite these virulence mechanisms, most humans carry *S. aureus* as a commensal; establishment of invasive disease requires breaks in mucosal or integumental surfaces (13, 14).

*C. albicans* is also a commensal of humans, colonizing the gut, skin, and mucosal surfaces, but can act as a pathogen colonizing medical devices, such as dentures and catheters (15, 16). This polymorphic fungal pathogen can detect changes in environmental parameters and shift from the single-cell yeast morphology to the multicellular hyphal morphology. Using epithelial receptors and secreted factors, hyphae can actively penetrate mucosal barriers (17, 18). The dysfunction of immune functions related to systemic conditions, such as HIV infection/AIDS, cancer, and immunosuppression for organ transplant, enables this fungus to transition into an invasive pathogen, causing bloodstream infections with a high rate of mortality (19–21). The rate of oral candidiasis in AIDS and cancer patients is 9 to 31% and 20%, respectively (8, 22). As the frequency of *Candida* strains resistant to azole- and echinocandin-class drugs increases, the direct hospitalization costs are predicted to increase by millions of U.S. dollars annually (23).

*S. aureus* and *C. albicans* have been coisolated from patients with a range of biofilm-associated diseases, from noninvasive colonization of denture surfaces leading to tissue inflammation (denture stomatitis) to complex and life-threatening burn-wound infections, ventilator-associated pneumonia, and cystic fibrosis (24–28). Both organisms are consistently isolated from bloodstream infections (4, 8, 29–31), and up to 24% of patients with confirmed candidemia have concurrent bacteremia; *S. aureus* was isolated in 20% of these cases (32). As Klotz and colleagues noted, detection of candidemia is difficult, with most inquiries underestimating the true burden of disease; these clinical findings suggest that *C. albicans* is a risk factor for *S. aureus* bacteremia and that their synergistic interaction increases mortality rates (32).

We have investigated the mechanisms of the *C. albicans* and *S. aureus* association and reported that *S. aureus* can strongly adhere to *C. albicans* hyphae (33). This specific interaction is mediated by the Als3p protein of *C. albicans* (34) and is expressed exclusively in the hyphal morphology (35). These studies, as well as others, suggest that both organisms benefit from this interaction, which may modulate the host immune response differently than monospecies infections. Peters and Noverr (2013) utilized a murine model to compare monospecies and polymicrobial (*C. albicans* and *S. aureus*) peritonitis, the incidence of which is rising due to the increased use of peritoneal dialysis (36). Their results demonstrated increased neutrophil trafficking into the peritoneal cavity and heightened levels of proinflammatory cytokines associated with innate immune responses, including interleukin-6 (IL-6) and granulocyte colony-stimulating factor. However, the immunological mechanisms and signaling behind this infectious synergy remain unclear.

Using an established murine model of oral coinfection, we showed that a physical interaction between *C. albicans* hyphae and *S. aureus* is required for bacterial invasion (37). The association of *S. aureus* with Als3p-expressing *C. albicans* in the oral cavity resulted in *S. aureus* bacteremia and the isolation of *S. aureus* bacteria from kidney tissue. Histology demonstrated that *C. albicans* hyphae penetrated the tongue epithelium and that *S. aureus* comigrated with the hyphae. Therefore, we proposed the following hitchhiking hypothesis: *S. aureus* adhesion to *C. albicans* hyphae (mediated by Als3p) enables *S. aureus* to utilize the invasive potential of *C. albicans* (37). However, *S. aureus* rarely adheres to the growing tip of *Candida* hyphae and remains static as the hyphae grow at their tip, growth that mimics the traversal of epithelial layers of the tongue (see Fig. S1 in the supplemental material).

*S. aureus* can take up residence within phagocytes, such as macrophages and neutrophils, and persist at low levels until escaping (38–40). *S. aureus* can also replicate and survive within liver macrophages (Kupffer cells) by preventing macrophages from using reactive oxygen species (ROS) to clear the infection (40). Therefore, we now hypothesize that host phagocytic cells are recruited to the highly immunogenic *C. albicans* hyphae but are unable to engulf the relatively large (>20  $\mu\text{m}$ ) hyphal ele-

ments. Instead, hypha-attached *S. aureus* cells are easily taken up by activated phagocytes and disseminated systemically, resulting in infection. Thus, *S. aureus* may subvert the compromised oral innate immune system in critically ill patients and use phagocyte mobility to spread to other organs, causing infections that result in significant morbidity and mortality in those with immune dysfunction.

In this study, we examined the hypothesized mechanism by which *C. albicans* hyphae facilitate bacterial dissemination by analyzing *in vitro* phagocytosis by macrophages and neutrophils in the presence of *S. aureus* and *C. albicans* by time-lapse microscopy. Using our murine model of oral coinfection, we demonstrate that the draining cervical lymph nodes can function as a reservoir for *S. aureus* during coinfection. Our results suggest that the interaction between *S. aureus* and *C. albicans* enables the former to hitchhike within the innate phagocytic immune response and that the oral cavity can be an intrinsic portal for systemic disease.

## RESULTS

***S. aureus* does not travel along growing *C. albicans* hyphae.** To evaluate how nonmotile *S. aureus* can utilize *C. albicans* to traverse epithelial tissue, we used time-lapse microscopy to visualize the association of *S. aureus* with *C. albicans*. We found that as hyphae extended at their tips, adherent *S. aureus* did not travel along the length of the hypha but remained at the initial attachment site (Fig. 1A; see also Video S1 in the supplemental material). This suggests that *S. aureus*, when it is strongly bound to Als3p on hyphae of *C. albicans*, does not travel alongside the growing hypha and may not utilize the penetrating potential of *C. albicans* hyphae to traverse epithelial tissue. In addition, under conditions simulating venous blood flow, *S. aureus* remained firmly attached to *C. albicans* (Video S2), preventing dissemination through the host.

**Innate immune cells are highly attracted to *C. albicans* yet phagocytose *S. aureus*.** Previous research has shown that innate immune cells, particularly macrophages, can attempt to engulf *C. albicans* yeast blastospheres but that this action triggers hyphal formation, leading to macrophage death (41, 42). Strikingly, phagocytes are generally more attracted to hyphae than to yeast cells due to significant differences in cell wall composition, including glucan production and expression (43). The adhesion forces of *S. aureus* on the hyphae of *C. albicans* are particularly strong (44); this prompted us to ask the question whether *S. aureus* strongly bound to the hyphae of *C. albicans* is protected against phagocytosis. We sought to determine if this occurs following the introduction of macrophages to *C. albicans* hyphae to more accurately simulate an innate immune response in the host. J774 murine macrophages applied to coculture immediately targeted hyphae (Fig. 1B; time zero) but clung to the appendage as they reached out to grab nearby green fluorescent protein (GFP)-labeled *S. aureus* (Fig. 1B; time  $T = 18$  min and  $T = 54$  min). Macrophages were capable of removing a significant amount of adherent *S. aureus* bacteria for a prolonged period (72 min) and climbed extending hyphae to reach distant bacteria (Fig. 1B, bottom,  $T = 54$  and 72 min, and Video S3).

The interaction between *S. aureus* and surface interfaces, including *C. albicans* hyphae, can be modified by addition of fetal bovine serum (FBS). On polystyrene (PS) surfaces, serum inhibits the adhesion of *S. aureus* to most surfaces but not to *C. albicans* hyphae (45). Introduction of large quantities of serum ( $>25\%$ ) to hyphae results in the nonspecific binding of *S. aureus* and *C. albicans* (34, 46). We used the differential effect that serum has on the interaction of *S. aureus* with hyphae and PS surfaces to gain insight into the preference of macrophages for hypha-bound *S. aureus* or PS surface-bound *S. aureus*. Macrophages preferentially sought out hyphae irrespective of the presence of serum, and by 6 h, most macrophages were attached to hyphae (Fig. 1C and D, middle, black bars versus gray bars). Similar to previous results, we noted that *S. aureus* binding to *C. albicans* increased with just the addition of 10% serum (Fig. 1C and 1D, left). In the absence of serum, with *S. aureus* adhering to both PS surfaces and hyphae, macrophages preferably phagocytosed *Candida*-adherent *S. aureus* (Fig. 1D, left; the data are quantified in Fig. 1D, right) rather than surface-adherent *S. aureus*.

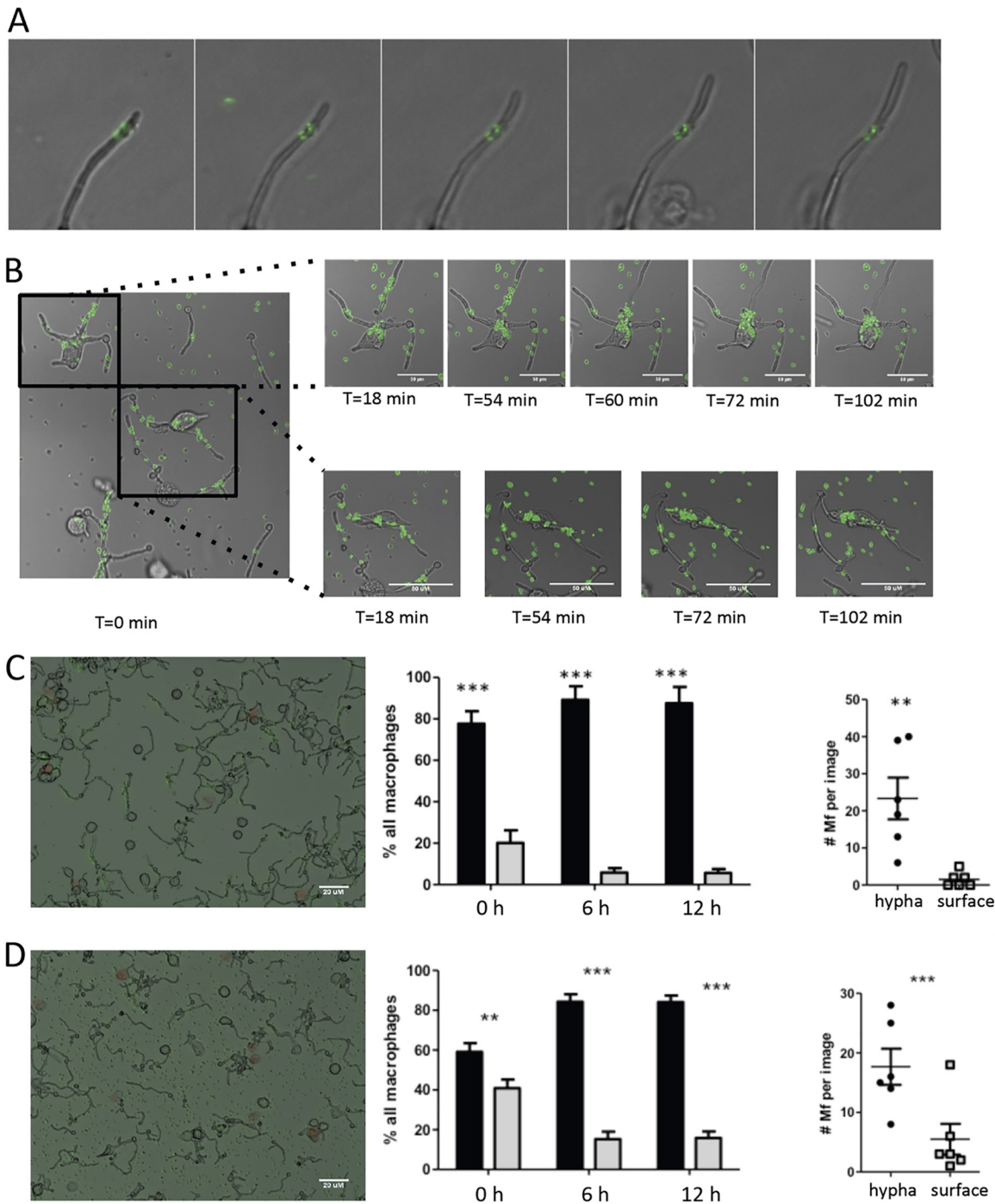


**FIG 1** *S. aureus* cells remain adherent to a single point on *C. albicans* hyphae in coculture *in vitro*. (A) Time-lapse microscopy was used to visualize *S. aureus* adhering to growing hyphae of *C. albicans*. (B) Active phagocytosis of adherent *S. aureus* from the hyphae of *C. albicans* was monitored for over 1 h after the introduction of macrophages. Macrophages can be seen extracting *S. aureus* from distant areas (top series) or crawling along hypha and removing nearby *S. aureus* (bottom series). (C) The impact of serum on immune cell targeting was tested by coating with 10% serum prior to macrophage application. In total, macrophages preferentially attached to *C. albicans* hyphae (center, black bars) over PS (center, gray bars), and after 6 h, 90% of all macrophages were attached to hyphae, where phagocytic activity occurred. Within individual views, an average of 25 macrophages (Mf) could be seen attaching to hyphae (right, black dots) and only a select few were detected still attached to PS (right, open squares). (D) The absence of serum did not impact the phagocytosis of *S. aureus* on the hyphae of *C. albicans*. Actively phagocytosing macrophages were scored relative to their hypha-associated state (center, black bars, and right, black dots) or surface-associated state (center, gray bars, and right, open squares). Bars = 20  $\mu$ m. *P* values were determined by Student's *t* test. \*\*, *P* < 0.001; \*\*\*, *P* < 0.0001.

These data suggest that macrophages are primarily recruited by *C. albicans* hyphae, leading or even facilitating the phagocytosis of hypha-adherent *S. aureus*.

***S. aureus* escapes the oral cavity by traversing draining cervical lymph nodes.**

*S. aureus* typically requires a portal of entry, i.e., a breach of mucosal or skin integrity, to cause life-threatening disease (14). In light of our *in vitro* observations using a macrophage cell line, we used our murine model of oral coinfection to determine whether phagocytes facilitate staphylococcal dissemination. As described previously (37), using corticosteroid injections, we achieved consistent immunosuppression of C57BL/6 mice, which enabled colonization by *C. albicans*, with and without *S. aureus*, of the tongue tissue (Fig. 2A). This colonization was stable 1 and 2 days after coinfection with *S. aureus* (Fig. 2B). We noted persistent and heavy *S. aureus* infection of underlying tongue tissue only in the coinfecting mice, supporting previous findings that *S. aureus* cannot actively penetrate the tongue epithelium (i.e., an intact mucosal barrier), requiring the presence of *C. albicans* (37).

Viable *S. aureus* was detected exclusively in the draining cervical lymph nodes, which handle the lymph circulation for the oral cavity, of coinfecting mice (Fig. 2C). Similarly, *S. aureus* disseminated into the kidney tissue only of coinfecting mice, and coinfecting mice that lacked disseminated disease also had no viable *S. aureus* in their lymph nodes (Fig. 2D). Fluorescence-activated cell sorting (FACS) analysis of lymph node cells of uninfected and coinfecting mice gated on macrophages (F4/80 marker) and neutrophils (Ly6G marker) showed that those of coinfecting mice contained intracellular *S. aureus* (Fig. 2E). At 1 and 2 days post-*S. aureus* infection, the bacterial burdens in both the lymph nodes and kidneys increased (Fig. 2F and G), demonstrating the temporal progression of *S. aureus* infection from the cervical lymph nodes to the kidneys. Mice infected solely with *S. aureus* had no lymph node or kidney bacterial burdens, supporting the findings of our previous studies that coinfection must be present for systemic disease (37). Taken together, these data support a role for host phagocytes in the development of systemic staphylococcal disease following oral coinfection by *S. aureus* and *C. albicans*.

**Phagocytic cells converge on *C. albicans* hyphae *in vivo* early in infection and cause inflammatory destruction of the tongue structure.** To link our earlier *in vitro* observations with the *in vivo* attraction of phagocytic cells by *C. albicans*, we used immunohistochemistry to visualize the impact of coinfection on tongue tissue and its innate defenses. We stained uninfected and infected tongue tissue sections from our murine model with periodic acid-Schiff (PAS) stain and counterstained with hematoxylin for nuclei. PAS stain stains the glucans and carbohydrates that compose fungal membranes, allowing the visualization of both yeast and hyphae. The overall tongue musculature was strikingly different between uninfected (Fig. 3A and B) and coinfecting (Fig. 3C to F) mice. The loss of keratinized tissue peaks was prominent in coinfecting mice, and the deep muscular layers of the tongue were highly disrupted, showing evidence of inflammation (Fig. 3C and D). Uninfected mice showed few inflammatory cells in the keratinized epithelium and muscle layers (Fig. 3A and B). Closer examination of infected tissue 1 day after coinfection demonstrated infiltration of polymorphonuclear leukocytes (PMNs) throughout the muscular layers and into the squamous epithelium on the dorsum of the tongue (Fig. 3D, red arrows). Bacterial clumps were associated with the hyphae of *C. albicans*, even at the early stages of infection (Fig. 3E, red box), and PMNs and monocytes were observed to be swelling and phagocytizing staphylococci (Fig. 3F, red boxes and red arrows). Immunohistochemical labeling of macrophages in tongue tissue at 5 days postinfection showed these cells actively engulfing the *S. aureus* bacteria within the keratinized layer (Fig. 3G and Fig. S4). Confocal imaging focusing on single macrophages demonstrated *S. aureus* within anti-CD68-labeled macrophages from orthogonal projections (Fig. 3G, bottom). These images provide support for the suggestion that, *in vivo*, phagocytes are attracted by *C. albicans* and can act as reservoirs for *S. aureus*, enabling the bacteria to access multiple organ systems in the host.



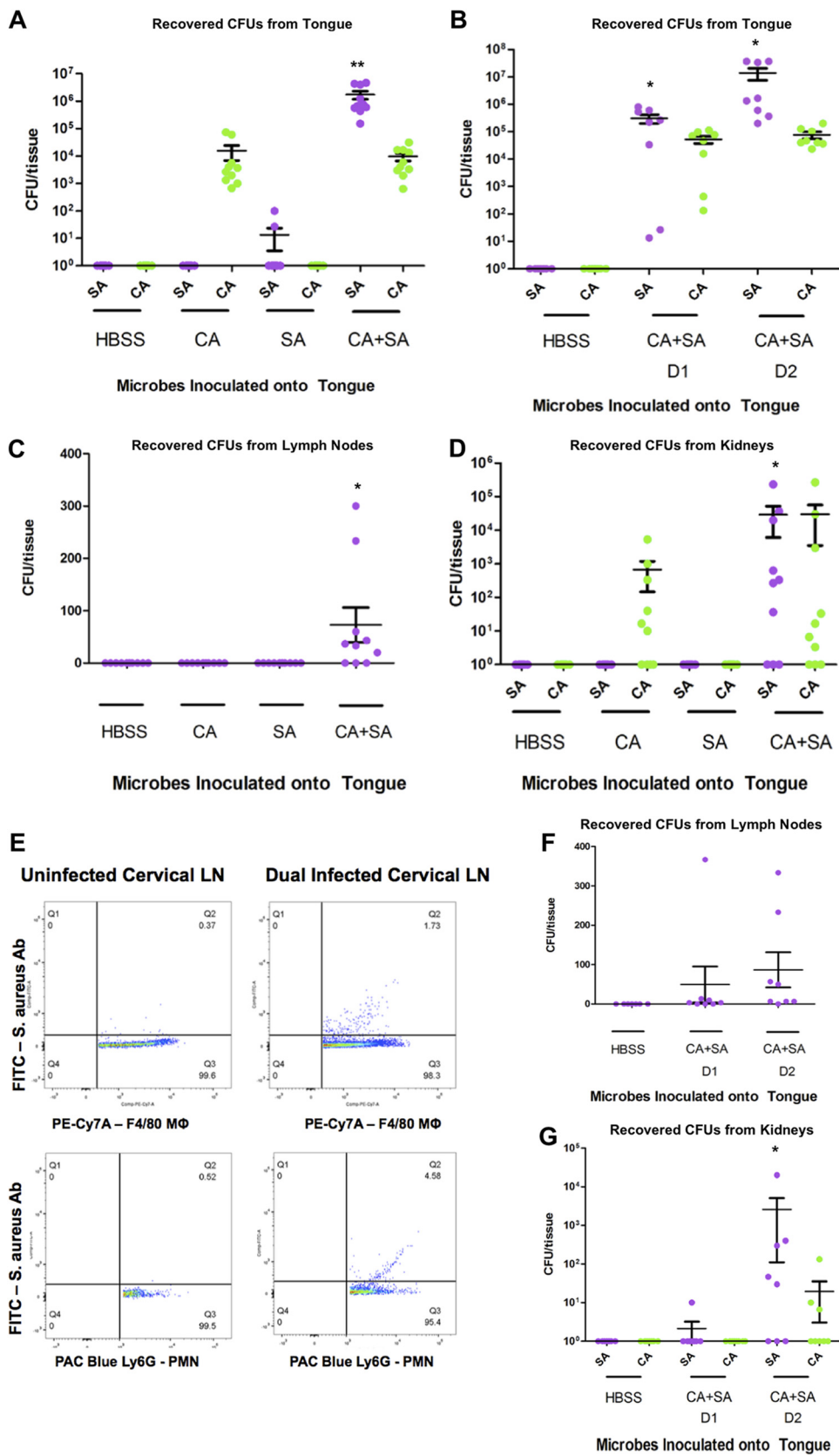


**FIG 2** *In vivo* oral coinfection demonstrates trafficking of phagocytes from tongue tissue to draining cervical lymph nodes and progression of systemic MRSA infection. (A and B) Numbers of CFU in tongue tissue following administration of Hanks balanced salt solution (HBSS), *Candida albicans* SC5314 alone (CA), methicillin-resistant (Continued on next page)

## DISCUSSION

In this study, we revisited our previous hypothesis that *C. albicans* facilitates staphylococcal disease by a mechanism of bacterial hitchhiking (37). We observed *in vitro* that adherent *S. aureus* does not progress with hyphal extension, thereby eliminating the possibility that staphylococci are actively transported through tissue as a bacterial hitchhiker. When phagocytic cells, the first lines of defense against infection, were added to these *in vitro* cultures, macrophages were highly attracted to *C. albicans* hyphae yet selectively engulfed the hypha-attached *S. aureus*. Therefore, we hypothesized that *in vivo*, highly immunogenic *C. albicans* hyphae attract phagocytic cells, which mediate staphylococcal uptake and dissemination, essentially providing *S. aureus* with a *porte d'entrée*.

To test this hypothesis, we used our established model of oral coinfection in immunocompromised C57BL/6 mice (37). FACS analysis of macrophages and neutrophils revealed intracellular *S. aureus* cells within the lymph nodes of only those hosts with oral coinfection with both *S. aureus* and *C. albicans*. Culture of lymph nodes from coinfecting hosts showed that these phagocyte-associated staphylococci were viable. In addition, the data indicated a temporal progression of infection from the cervical lymph nodes to the kidneys. Finally, we visualized macrophages actively engulfing *S. aureus* in tongue tissue using immunohistochemistry and confocal microscopy. These results provide evidence that *S. aureus* bacteria attached to *C. albicans* hyphae are phagocytosed and are transported in this protected intracellular environment to distal host sites, promoting disseminated staphylococcal disease.

Macrophages are highly attracted to *C. albicans*, and the fungus is capable of inhibiting their respiratory burst by secreting molecules to disable nitric oxide production and alkalinizing the macrophage intracellular pH through fungal ammonia production, preventing fungal death. This allows engulfed yeast to transition into hyphae, perforate the phagosome, and escape back into the extracellular environment (41, 42, 47, 48). Multiple studies have previously shown the plasticity of the survival responses from *C. albicans* in the presence of macrophages through *in vitro* experiments; these studies focused on how yeast cells within a macrophage rely on transcription factors encoding amino acid metabolism to sense the phagosome environment and, in turn, induce hyphal formation (42, 48). Our *in vitro* studies aimed to examine how this interaction would change if the macrophage encountered penetrating hyphae and bacteria, representing invasion through tongue tissue, as seen in oropharyngeal candidiasis. Instead of hyphae perforating the immune cell and killing it, macrophages used the hyphae as a scaffold and targeted attached *S. aureus* (Fig. 1). This interaction was not inhibited by the exclusion of serum (Fig. 1C and D). These findings suggest that in the interaction of *C. albicans* with *S. aureus*, attraction of macrophages by hyphae facilitates phagocytosis of attached bacteria.

In mice with oral coinfection, we found viable *S. aureus* colonizing the lymph nodes and kidneys, suggesting that phagocytes do not kill *S. aureus* upon endocytosis of attached bacteria (Fig. 2C and D). We did not find viable *C. albicans* within lymph nodes, possibly due to an inability of macrophages and neutrophils to engulf large hyphal segments that would be present from an established case of candidiasis. Macrophage-mediated phagocytosis of bacteria is associated with the release of oxygen radicals into the phagosome to create an inhospitable environment (49). This oxidative burst is a

### FIG 2 Legend (Continued)

*Staphylococcus aureus* USA300 alone (SA), or *Candida albicans* SC5314 alone and methicillin-resistant *Staphylococcus aureus* USA300 (CA+SA) to the oral cavity of C57BL/6 mice at 1 to 2 days (B) or 3 days (A) following oral inoculation of *S. aureus*. (C and D) Numbers of CFU in the draining cervical lymph nodes (C) and kidneys (D) at 3 days post-oral inoculation with *S. aureus*. (E) Flow cytometry analysis of cervical lymph node (LN) cell suspensions following fixation, host macrophage (PE-Cy7A-F4/80) or neutrophil (Pacific Blue [PAC Blue]-Ly6G) antibody labeling, permeabilization, and methicillin-resistant *S. aureus* (FITC-*S. aureus* antibody [Ab]) labeling 3 days following oral inoculation of uninfected controls or *S. aureus* and *C. albicans* dual species-infected mice. (F and G) Numbers of CFU in cervical lymph nodes (F) and kidneys (G) at 1 to 2 days postinoculation of *S. aureus*. *P* values were determined by one-way analysis of variance with Dunnett's multiple-comparison test. \*,  $P < 0.05$ ; \*\*,  $P < 0.001$ .

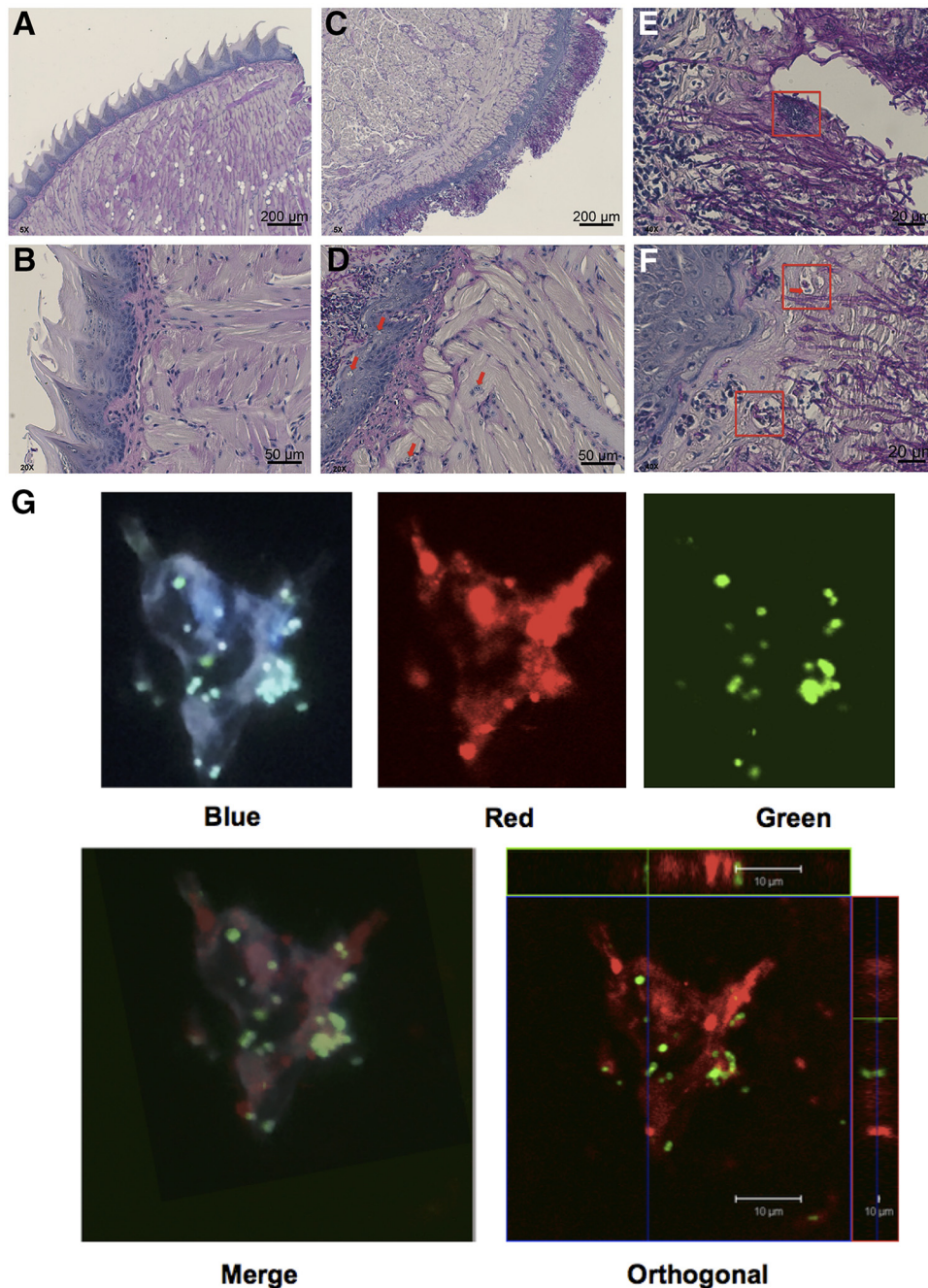


**FIG 3** Innate immune cells enter tongue tissue to colocalize at hyphae and bacteria within 1 day of coinfection. Tongues were excised from immunocompromised animals, embedded in paraffin, and stained with PAS. Images represent tongues from two uninfected mice (A and B) and two infected mice (C and D) at 1 day after coinfection with *S. aureus* and *C. albicans*. Red arrows indicate PMN invasion up hyphae (D), and red boxes indicate staphylococci clumping tightly with *C. albicans* hyphae and cells (E) or monocytes surrounding hyphae to seize bacteria (F; the red box and the red box with a red arrow indicate ingested staphylococci). Magnifications,  $\times 5$  (A and B),  $\times 20$  (C and D), and  $\times 40$  (E and F). (G) Immunohistochemically labeled macrophages (red filter) were seen engulfing *S. aureus* (green filter) only in coinfecting mice. The fluorescent images were counterstained with DAPI to show nuclei (blue filter). An orthogonal image (bottom right) shows *S. aureus* within a macrophage. Magnifications,  $\times 100$ .

vital component of innate immunity against bacteria (50). To sustain candidiasis, we administered corticosteroid injections to the mice prior to infection. The usage of corticosteroids remains common practice for transplant patients to prevent graft-versus-host disease and increases the risk of oropharyngeal and disseminated candidiasis in these patients (19). The impacts of corticosteroids on the immune system have



long been explored; rat studies have shown that their application dampens immune responses and impairs the activity of alveolar macrophages against bacteria (51). In particular, IL-1 $\beta$  signaling is downregulated during corticosteroid usage, decreasing the effectiveness of the respiratory burst in these innate immune cells (52). Sureward and colleagues (2016) noted that the loss of NADPH oxidase through the use of *Ncf1*<sup>m1J</sup> and *Cybb*<sup>-/-</sup> knockout mouse strains prevented innate immune cells from producing the needed reactive oxygen species and allowed MRSA to replicate to high levels in Kupffer cells of otherwise immunocompetent animals during intravenously induced *S. aureus* bacteremia (40). Only by fusing the antibiotic vancomycin to liposomes to make “vancosomes” that could be taken up by macrophages were the authors able to decrease liver colonization and increase survival (40). The intracellular survival of *S. aureus* has been described in macrophages and PMNs in immunocompetent hosts using *in vitro* and *in vivo* monospecies infections (reviewed in references 53 and 54). It is likely that in our mice, the macrophages and neutrophils that engulf *S. aureus* cells no longer function optimally, further enhancing the probability of bacterial survival. This finding, together with previous reports of the difficulty of treating pathogens hidden within these cells, is of great clinical importance (40, 55). *S. aureus* and *C. albicans* are often coisolated from immunocompromised patients (28, 32), and the coculture of both organisms from the blood is associated with a 50% mortality rate. This finding also suggests that treatment of polymicrobial infections may require targeting of immune cells to prevent reseeding after antibiotic treatment.

Our previous studies have established that Als3p expression by *C. albicans* is required for the binding of *S. aureus* and the subsequent dissemination from the oral cavity to distant organs, such as the kidney (34, 37, 56). Als3p is not the only mechanism of staphylococcal adherence to *C. albicans*, as others have noted that nonspecific interactions can be introduced by high levels of serum (46, 57), suggesting that serum components can assist with the binding between these pathogens. In the serum-limited oral cavity, such nonspecific binding is unlikely to occur; moreover, we demonstrated here that the interaction between *C. albicans* and *S. aureus* is strong and is unbroken by conditions simulating blood flow (see Fig. S2 in the supplemental material). As such, adherent bacteria could survive as hyphae traverse through tissue. However, we showed *in vitro* that attached bacteria are sedentary and are not passed along Als3p receptors or other binding mechanisms as the hyphae grow (Fig. 1A and Fig. S1). Therefore, *C. albicans* hypha formation does not represent a direct transport mechanism for *S. aureus* but, rather, represents a method to start infection and recruit macrophages into epithelial tissue. This is further supported by the massive inflammation at the epithelial border of the tongue (Fig. 3D and F) and confocal imaging of internalized *S. aureus* within tongue macrophages (Fig. 3G and Fig. S3). How *S. aureus* escapes the macrophage after phagocytosis during polymicrobial infection is unknown, but this bacterium possesses several leukocidins and toxins that can lyse cells (58). Identification of the staphylococcal factors that promote survival during the innate immune response will be the focus of future studies.

Phagocytosis is a complex process involving an interplay between phagocytic receptors and pattern recognition receptors (PRRs) that detect broad classes of pathogens (59). Initially, phagocytes are recruited to mucosal surfaces infected by *Candida* under the direction of host antimicrobial peptides (e.g.,  $\beta$ -defensin 2) and chemokines (e.g., CCL20) (60–63). Phagocytes recognize the pathogen-associated molecular patterns (PAMPs), including *N*-linked and *O*-linked mannans and  $\beta$ -glucans, present on the fungal cell wall through host PRRs and attach to hyphae (64–67). Following this recognition, the relatively large hyphae are not effectively phagocytosed. However, the PAMPs (including peptidoglycan, lipoteichoic acid, and lipoproteins) of the hypha-adherent *S. aureus* bacteria are also readily identified by the host PRRs. The signaling pathways within host phagocytes that are influenced during phagocytosis of coinfecting *C. albicans* and *S. aureus* remain largely unknown. Extracellular ATP is recognized as a danger signal, released upon infection or cell death. Pérez-Flores and colleagues (2016) showed that extracellular ATP and Ca<sup>2+</sup> play a role in phagocytosis by coating

nanoparticles with *S. aureus* or live *Candida glabrata* yeast cells and feeding them to murine macrophages in the presence of exogenous ATP and  $\text{Ca}^{2+}$  (68). Membrane ionotropic P2X receptor 1 (P2X1) to P2X7 sense danger molecules, such as ATP, and P2X7 is abundant on the surface of macrophages (69). Activation of P2X7 is important in the response to infections caused by intracellular bacteria (70, 71). Pérez-Flores et al. reported that activation of P2X7 inhibited the phagocytosis of bacteria but not *C. glabrata* by J774 macrophages (68). This supports the notion that P2X receptors are required to sense the cellular damage caused by a bacterium-fungus coinfection and initiate the immune response. However, the mechanisms of phagocytosis, intracellular survival, and phagocytic escape of *S. aureus* during coinfection remain to be elucidated. Therefore, future studies will focus on the blockade of phagocyte signaling and its impact on bacterial dissemination during coinfection.

In summary, *C. albicans* hyphae attract phagocytes that target attached *S. aureus* cells, which are actively removed from these hyphae and phagocytosed by macrophages and PMNs. Following ingestion, *S. aureus* escapes intracellular killing and is trafficked to the draining host lymph nodes and further distal sites, resulting in life-threatening disseminated infections. To our knowledge, this is the first report of a critical role for the innate immune system in promoting the development of systemic disease following polymicrobial infection of the oral cavity. The impact of these findings reaches beyond *S. aureus* and *C. albicans* interactions at the oral mucosal surfaces. These findings may be applicable to other mucosal surfaces where these microbes coexist (e.g., the craniofacial, respiratory, gastrointestinal, and urogenital tracts) as well as in infections associated with indwelling medical devices (e.g., intravenous catheters, ventilator tubes), burn wounds, or local host immune dysfunction (e.g., diabetic foot ulcers, traumatic musculoskeletal infections, or decubitus ulcers). It is also possible that the oral innate immune cells transport periodontal pathogens, as periodontal disease is correlated with systemic diseases, such as diabetes, atherosclerosis, myocardial infarction, and stroke, with periodontal pathogens being detected in atherosclerotic and cardiac lesions (72–78). However, the direct implications of periodontal pathogens in these diseases remain debated, and further study is needed. Regardless, the results of this study highlight the importance of studying the systemic implications of localized polymicrobial infections as well as the complicity of the host immune response in the infectious synergism seen in some polymicrobial infections.

## MATERIALS AND METHODS

**Strains and growth conditions.** *Candida albicans* strain SC5314 (79) was maintained from glycerol freezer stocks on yeast-peptone-dextrose agar. Methicillin-resistant *Staphylococcus aureus* (MRSA) strain USA300 JE2, from the Network on Antimicrobial Resistance in *Staphylococcus aureus* (NARSA) (80), was maintained from glycerol freezer stocks on sheep's blood agar (BBL). GFP-labeled *S. aureus* ATCC 12600 (81) was used for *in vitro* assays and grown in brain heart infusion (BHI) broth supplemented with tetracycline (10  $\mu\text{g}/\text{ml}$ ; Sigma-Aldrich) at 37°C. For *in vitro* assays, *C. albicans* was grown in BHI broth at 30°C at an oblique angle to ensure growth in the yeast form only.

For animal studies, single colonies of *C. albicans* were grown in BHI broth (Teknova) supplemented with 10  $\mu\text{g}/\text{ml}$  chloramphenicol (Sigma-Aldrich) and subcultured for 3 days prior to inoculation into mice to ensure the presence of yeast blastospores. Cultures were grown at 30°C with shaking at 225 rpm under aerobic conditions and on the day of inoculation were washed and diluted to  $6 \times 10^6$  CFU/ml in Hanks balanced salt solution (HBSS). Single colonies of *S. aureus* JE2 were grown in Trypticase soy broth (TSB; Remel) overnight at 37°C and subcultured on the day of inoculation to mid-log phase. Cultures were washed and diluted to  $6 \times 10^6$  CFU/ml in HBSS. All inocula were kept at 30°C (*C. albicans*) or 37°C (*S. aureus*) prior to infection and were enumerated using serial dilution and viable counting.

**J774 macrophages.** J774 murine macrophages (ATCC TIB-67) were maintained in Dulbecco's modified Eagle's medium (DMEM) with 10% fetal bovine serum (FBS; Sigma-Aldrich) and an antibiotic-antimycotic solution (100 U/ml penicillin, 100  $\mu\text{g}/\text{ml}$  streptomycin, and 250 ng/ml amphotericin B [PSA]; Sigma-Aldrich). For phagocytosis assays, 80% confluent macrophages were removed from the culture flasks using a sterile cell scraper and diluted 10-fold in DMEM–10% FBS without PSA. To determine macrophage viability during assays, 0.2  $\mu\text{l}/\text{ml}$  propidium iodide (PI; Molecular Probes, Life Technologies) was added to diluted suspensions of macrophages.

***In vitro* phagocytosis.** Overnight cultures of *C. albicans* were diluted to an optical density at 600 nm ( $\text{OD}_{600}$ ) of ~0.003 in phosphate-buffered saline (PBS; Gibco BRL). Tissue culture-treated 12-well plates were seeded with 1 ml *C. albicans* suspension (Greiner Bio-One) and incubated for 3 h at 37°C to allow initial attachment and hyphal growth. After 3 h, the wells were washed with PBS and coated with serum

(1 ml of 50% FBS diluted in PBS) or PBS alone (1 ml) for 1 h. Following coating, the wells were washed with PBS and 1 ml of GFP-labeled *S. aureus* suspension diluted to an OD<sub>600</sub> of ~0.01 in PBS was added. *C. albicans* and *S. aureus* were then incubated for 1 h under gentle agitation to allow *S. aureus* to adhere to hyphae. Nonadherent *S. aureus* cells were removed by vigorous washing in PBS twice, and 1 ml of diluted (1:10) macrophage suspension in DMEM–10% FBS with or without PI was added. This dilution was determined to yield approximately 10<sup>5</sup> cells/ml. The plates were immediately placed under a microscope to visualize phagocytosis.

**Time-lapse microscopy. (i) Confocal microscopy.** The plates were placed under a Leica IR-BE infrared confocal microscope (Leica Microsystems) at room temperature. Phase-contrast and fluorescence images were acquired at 6-min intervals for 100 min, and z-stacks were created to span single-cell layers (8 μm). Images were processed using Leica Confocal software (Leica Microsystems) and ImageJ software (<http://imagej.nih.gov/ij/>).

**(ii) Inverted fluorescence microscopy.** Plates were placed under an Axio Observer Z1 automated microscope in a heated (37°C) plate holder (Zeiss). *C. albicans* and macrophages were visualized using bright-field illumination, *S. aureus* was visualized by imaging the GFP signal, and viability was monitored by PI staining. Images of at least two randomly selected fixed plate positions per experimental condition per run were taken every 10 min. Macrophages were imaged at a ×20 magnification for a maximum of 12 h. PI staining showed that 75% of the macrophages remained viable at 12 h, while most PMNs had died after 6 h. The obtained images were further processed using Montage software (Molecular Devices) and ImageJ software (<http://imagej.nih.gov/ij/>).

**(iii) Quantification of macrophages.** To calculate the percentage of macrophages adhering to hyphae or plastic, macrophages in time-lapse stack images were counted at three time points: 1 (0 min), 37 (6 h), and 73 (12 h). Their positions and viability were determined and divided by the total number of cells per image. The numbers of actively phagocytosing macrophages were determined by creating time-lapse movies from stack images and counting the number of active cells per movie. Quantification was performed in six independent experiments, using images from at least two different plate positions per experimental condition. Comparisons of the macrophage location between treated plates and hyphae were performed using Student's *t* test (two-tailed, unequal variance).

**Murine model of oral coinfection.** The murine immune response to a dual-species infection was tested using an oral coinfection model as described previously (37), with some modifications (see Fig. S5 in the supplemental material). The animal studies were approved by the University of Maryland Institutional Animal Care and Use Committee. Briefly, C57BL/6 mice were obtained from The Jackson Laboratory (Bar Harbor, ME) and maintained under pathogen-free conditions. Mice were given water treated daily with ampicillin (300 μg/ml) to reduce oral flora carriage and three subcutaneous shots of cortisone acetate (225 mg/kg of body weight) to suppress their immune system. Cortisone shots were given 1 day prior to the first inoculation (day 1) and every other day (days 3 and 5) thereafter to ensure continuous immunosuppression. The animals were anesthetized and laid supine while receiving a calcium alginate swab soaked in a *C. albicans* suspension (day 2) or an *S. aureus* suspension (day 4) for 75 min. Mice in the dual-species infection groups were inoculated on both days and, along with *S. aureus*-inoculated mice, were exposed to *S. aureus* (6 × 10<sup>6</sup> CFU/ml) in the drinking water for the remainder of the study. On day 6 or 7, depending on weight loss, mice were euthanized and their tongues, lymph nodes, and kidneys were harvested. A 2-mm slice of tongue was removed for determination of the microbial burden (number of CFU per tissue specimen). All tissues were homogenized in 500 μl of sterile PBS and serially diluted on CHROMagar for *S. aureus* and *C. albicans*. A total of 40 mice (10 mice per experimental condition) were used in three independent experiments (4 animals per group for 2 independent experiments, 2 animals per group for the immunofluorescence imaging independent experiment). Lymph nodes from uninfected and coinfecting mice (four mice per group) were pooled from a separate experiment for analysis via flow cytometry.

Lymph nodes were placed in cold sterile flow cytometry buffer (eBioscience), and cells were released by gentle grinding between two sterile frosted-glass microscope slides. Cells were pipetted repeatedly through a 25-gauge needle to produce single-cell suspensions. The suspensions were flushed through a 40-μm-pore-size basket filter and washed before being labeled with phycoerythrin (PE)-Cy7 conjugated to anti-F4/80 (clone BM8; BioLegend), Pacific Blue conjugated to anti-Ly6G (clone 1A8; BD Biosciences), and Alexa Fluor 674 conjugated to anti-CD11b (clone M1/70; BioLegend) for 1 h at 4°C. The cells were then washed and fixed for intracellular staining for 30 min at room temperature. Suspensions were permeabilized by incubating three times for 5 min each time with permeabilization buffer (eBioscience) at room temperature. Intracellular *S. aureus* was labeled using a fluorescein isothiocyanate (FITC)-conjugated anti-*S. aureus* antibody (polyclonal anti-rabbit immunoglobulin; GeneTex) and incubated for 30 min at room temperature. Cells were washed, resuspended in flow cytometry buffer on ice, and read on a Becton, Dickinson LSRII instrument using FACSDiva software. The populations were gated on macrophages and neutrophils to determine the presence of intracellular *S. aureus* bacteria using FlowJo software (Tree Star, Inc.).

**Tongue histology and immunohistochemistry.** Tongues were removed from euthanized uninfected mice and from mice euthanized 1 day after *C. albicans*-*S. aureus* infection. A small portion of tongue tissue was retained for CFU enumeration, and tongues were placed in neutral buffered formalin for paraffin embedding at the University of Maryland School of Medicine Pathology Associates. Sections were stained with periodic acid-Schiff (PAS) and examined by bright-field microscopy using a Zeiss Axio Imager microscope (Carl Zeiss). For immunohistochemistry, tongues were placed in Optimum Cutting Temperature (OCT) compound (Sakura Tissue-Tek) and snap-frozen in liquid nitrogen. Frozen tongue tissues were sectioned (10 μm) using a Leica AM1925 cryomicrotome and fixed in 4% paraformaldehyde

solution. Nonspecific staining was blocked with bovine serum albumin (BSA), and the slides were stained with an FITC-conjugated anti-*S. aureus* antibody (as used in flow cytometry) and an eFluor 660-conjugated anti-CD68 antibody (clone FA-11; eBioscience) overnight at 4°C. On the following day, the slides were washed in PBS and counterstained with DAPI (4',6-diamidino-2-phenylindole; ProLong Gold antifade mountant with DAPI; Molecular Probes), before being viewed under a Zeiss Meta confocal fluorescence microscope (Carl Zeiss) and analyzed using LSMIX software (Carl Zeiss).

## SUPPLEMENTAL MATERIAL

Supplemental material for this article may be found at <https://doi.org/10.1128/IAI.00137-19>.

**SUPPLEMENTAL FILE 1**, PDF file, 0.05 MB.

**SUPPLEMENTAL FILE 2**, PDF file, 0.1 MB.

**SUPPLEMENTAL FILE 3**, MOV file, 1.8 MB.

**SUPPLEMENTAL FILE 4**, AVI file, 0.05 MB.

**SUPPLEMENTAL FILE 5**, MOV file, 3.5 MB.

**SUPPLEMENTAL FILE 6**, MOV file, 0.6 MB.

**SUPPLEMENTAL FILE 7**, MOV file, 9.8 MB.

## REFERENCES

- Brogden KA, Guthmiller JM, Taylor CE. 2005. Human polymicrobial infections. *Lancet* 365:253–255. [https://doi.org/10.1016/S0140-6736\(05\)17745-9](https://doi.org/10.1016/S0140-6736(05)17745-9).
- Lynch AS, Robertson GT. 2008. Bacterial and fungal biofilm infections. *Annu Rev Med* 59:415–428. <https://doi.org/10.1146/annurev.med.59.110106.132000>.
- Deveau A, Bonito G, Uehling J, Paoletti M, Becker M, Bindschedler S, Hacquard S, Herve V, Labbe J, Lastovetsky OA, Mieszkin S, Millet LJ, Vajna B, Junier P, Bonfante P, Krom BP, Olsson S, van Elsas JD, Wick LY. 2018. Bacterial-fungal interactions: ecology, mechanisms and challenges. *FEMS Microbiol Rev* 42:335–352. <https://doi.org/10.1093/femsre/fuy008>.
- Lockhart SR, Etienne KA, Vallabhaneni S, Farooqi J, Chowdhary A, Govender NP, Colombo AL, Calvo B, Cuomo CA, Desjardins CA, Berkow EL, Castanheira M, Magobo RE, Jabeen K, Asghar RJ, Meis JF, Jackson B, Chiller T, Litvintseva AP. 2017. Simultaneous emergence of multidrug-resistant *Candida auris* on 3 continents confirmed by whole-genome sequencing and epidemiological analyses. *Clin Infect Dis* 64:134–140. <https://doi.org/10.1093/cid/ciw691>.
- Magill SS, Edwards JR, Bamberg W, Beldavs ZG, Dumyati G, Kainer MA, Lynfield R, Maloney M, McAllister-Hollod L, Nadle J, Ray SM, Thompson DL, Wilson LE, Fridkin SK, Emerging Infections Program Healthcare-Associated Infections and Antimicrobial Use Prevalence Survey Team. 2014. Multistate point-prevalence survey of health care-associated infections. *N Engl J Med* 370:1198–1208. <https://doi.org/10.1056/NEJMoa1306801>.
- Benito N, Franco M, Coll P, Gálvez ML, Jordán M, López-Contreras J, Pomar V, Monllau JC, Mirelis B, Gurguí M. 2014. Etiology of surgical site infections after primary total joint arthroplasties. *J Orthop Res* 32:633–637. <https://doi.org/10.1002/jor.22581>.
- Centers for Disease Control and Prevention. 2012. Active bacterial core surveillance report, Emerging Infections Program Network, methicillin-resistant *Staphylococcus aureus*, 2011. Centers for Disease Control and Prevention, Atlanta, GA.
- Morgan J, Meltzer MI, Plikaytis BD, Sofair AN, Huie-White S, Wilcox S, Harrison LH, Seaberg EC, Hajjeh RA, Teutsch SM. 2005. Excess mortality, hospital stay, and cost due to candidemia: a case-control study using data from population-based candidemia surveillance. *Infect Control Hosp Epidemiol* 26:540–547. <https://doi.org/10.1086/502581>.
- Kim J, Sudbery P. 2011. *Candida albicans*, a major human fungal pathogen. *J Microbiol* 49:171–177. <https://doi.org/10.1007/s12275-011-1064-7>.
- Mostofsky E, Lipsitch M, Regev-Yochay G. 2011. Is methicillin-resistant *Staphylococcus aureus* replacing methicillin-susceptible *S. aureus*? *J Antimicrob Chemother* 66:2199–2214. <https://doi.org/10.1093/jac/dkr278>.
- David MZ, Daum RS. 2010. Community-associated methicillin-resistant *Staphylococcus aureus*: epidemiology and clinical consequences of an emerging epidemic. *Clin Microbiol Rev* 23:616–687. <https://doi.org/10.1128/CMR.00081-09>.
- DeLeo FR, Otto M, Kreiswirth BN, Chambers HF. 2010. Community-associated methicillin-resistant *Staphylococcus aureus*. *Lancet* 375:1557–1568. [https://doi.org/10.1016/S0140-6736\(09\)61999-1](https://doi.org/10.1016/S0140-6736(09)61999-1).
- Acton DS, Plat-Sinnige MJ, van Wamel W, de Groot N, van Belkum A. 2009. Intestinal carriage of *Staphylococcus aureus*: how does its frequency compare with that of nasal carriage and what is its clinical impact? *Eur J Clin Microbiol Infect Dis* 28:115–127. <https://doi.org/10.1007/s10096-008-0602-7>.
- del Rio A, Cervera C, Moreno A, Moreillon P, Miro JM. 2009. Patients at risk of complications of *Staphylococcus aureus* bloodstream infection. *Clin Infect Dis* 48(Suppl 4):S246–S253. <https://doi.org/10.1086/598187>.
- Cannon RD, Chaffin WL. 2001. Colonization is a crucial factor in oral candidiasis. *J Dent Educ* 65:785–787.
- Budtz-Jorgensen E. 2000. Ecology of *Candida*-associated denture stomatitis. *Microb Ecol Health Dis* 12:170–185. <https://doi.org/10.1080/089106000750051846>.
- Phan QT, Fratti RA, Prasadarao NV, Edwards JE, Jr, Filler SG. 2005. N-cadherin mediates endocytosis of *Candida albicans* by endothelial cells. *J Biol Chem* 280:10455–10461. <https://doi.org/10.1074/jbc.M412592200>.
- Phan QT, Myers CL, Fu Y, Sheppard DC, Yeaman MR, Welch WH, Ibrahim AS, Edwards JE, Jr, Filler SG. 2007. Als3 is a *Candida albicans* invasin that binds to cadherins and induces endocytosis by host cells. *PLoS Biol* 5:e64. <https://doi.org/10.1371/journal.pbio.0050064>.
- Dongari-Bagtzoglou A, Dwivedi P, Ioannidou E, Shaqman M, Hull D, Bureson J. 2009. Oral *Candida* infection and colonization in solid organ transplant recipients. *Oral Microbiol Immunol* 24:249–254. <https://doi.org/10.1111/j.1339-302X.2009.00505.x>.
- de Repentigny L, Lewandowski D, Jolicoeur P. 2004. Immunopathogenesis of oropharyngeal candidiasis in human immunodeficiency virus infection. *Clin Microbiol Rev* 17:729–759. <https://doi.org/10.1128/CMR.17.4.729-759.2004>.
- Centers for Disease Control and Prevention. 1992. 1993 revised classification system for HIV infection and expanded surveillance case definition for AIDS among adolescents and adults. *MMWR Recommend Rep* 41(RR-17):1–19.
- Schelenz S, Abdallah S, Gray G, Stubbings H, Gow I, Baker P, Hunter PR. 2011. Epidemiology of oral yeast colonization and infection in patients with hematological malignancies, head neck and solid tumors. *J Oral Pathol Med* 40:83–89. <https://doi.org/10.1111/j.1600-0714.2010.00937.x>.
- Centers for Disease Control and Prevention. 2013. Antibiotic resistance threats in the United States, 2013. Centers for Disease Control and Prevention, Atlanta, GA.
- Cuesta AI, Jewtuchowicz V, Brusca MI, Nastro ML, Rosa AC. 2010. Prevalence of *Staphylococcus* spp and *Candida* spp in the oral cavity and periodontal pockets of periodontal disease patients. *Acta Odontol Latinoam* 23:20–26.
- Timsit JF, Cheval C, Gachot B, Bruneel F, Wolff M, Carlet J, Regnier B. 2001. Usefulness of a strategy based on bronchoscopy with direct examination of bronchoalveolar lavage fluid in the initial antibiotic



- therapy of suspected ventilator-associated pneumonia. *Intensive Care Med* 27:640–647. <https://doi.org/10.1007/s001340000840>.
26. Valenza G, Tappe D, Turnwald D, Frosch M, Konig C, Hebestreit H, Abele-Horn M. 2008. Prevalence and antimicrobial susceptibility of microorganisms isolated from sputa of patients with cystic fibrosis. *J Cystic Fibrosis* 7:123–127. <https://doi.org/10.1016/j.jcf.2007.06.006>.
  27. Baena-Monroy T, Moreno-Maldonado V, Franco-Martinez F, Adalpe-Barrios B, Quindos G, Sanchez-Vargas LO. 2005. *Candida albicans*, *Staphylococcus aureus* and *Streptococcus mutans* colonization in patients wearing dental prosthesis. *Med Oral Patol Oral Cir Bucal* 10(Suppl 1): E27–E39.
  28. Gupta N, Haque A, Mukhopadhyay G, Narayan RP, Prasad R. 2005. Interactions between bacteria and *Candida* in the burn wound. *Burns* 31:375–378. <https://doi.org/10.1016/j.burns.2004.11.012>.
  29. Klevens RM, Morrison MA, Nadle J, Petit S, Gershman K, Ray S, Harrison LH, Lynfield R, Dumyati G, Townes JM, Craig AS, Zell ER, Fosheim GE, McDougal LK, Carey RB, Fridkin SK, Active Bacterial Core Surveillance (ABCs) MRSA Investigators. 2007. Invasive methicillin-resistant *Staphylococcus aureus* infections in the United States. *JAMA* 298:1763–1771. <https://doi.org/10.1001/jama.298.15.1763>.
  30. Perloth J, Choi B, Spellberg B. 2007. Nosocomial fungal infections: epidemiology, diagnosis, and treatment. *Med Mycol* 45:321–346. <https://doi.org/10.1080/13693780701218689>.
  31. Kock R, Becker K, Cookson B, van Gemert-Pijnen JE, Harbarth S, Kluytmans J, Mielke M, Peters G, Skov RL, Struelens MJ, Tacconelli E, Navarro Torne A, Witte W, Friedrich AW. 2010. Methicillin-resistant *Staphylococcus aureus* (MRSA): burden of disease and control challenges in Europe. *Euro Surveill* 15(41):pii=19688. <https://doi.org/10.2807/ese.15.41.19688-en>.
  32. Klotz SA, Chasin BS, Powell B, Gaur NK, Lipke PN. 2007. Polymicrobial bloodstream infections involving *Candida* species: analysis of patients and review of the literature. *Diagn Microbiol Infect Dis* 59:401–406. <https://doi.org/10.1016/j.diagmicrobio.2007.07.001>.
  33. Peters BM, Jabra-Rizk MA, Scheper MA, Leid JG, Costerton JW, Shirliff ME. 2010. Microbial interactions and differential protein expression in *Staphylococcus aureus*-*Candida albicans* dual-species biofilms. *FEMS Immunol Med Microbiol* 59:493–503. <https://doi.org/10.1111/j.1574-695X.2010.00710.x>.
  34. Peters BM, Ovchinnikova ES, Krom BP, Schlecht LM, Zhou H, Hoyer LL, Busscher HJ, van der Mei HC, Jabra-Rizk MA, Shirliff ME. 2012. *Staphylococcus aureus* adherence to *Candida albicans* hyphae is mediated by the hyphal adhesin Als3p. *Microbiology* 158:2975–2986. <https://doi.org/10.1099/mic.0.062109-0>.
  35. Beaussart A, Alsteens D, El-Kirat-Chatel S, Lipke PN, Kuchariková S, Van Dijck P, Dufrene YF. 2012. Single-molecule imaging and functional analysis of Als adhesins and mannans during *Candida albicans* morphogenesis. *ACS Nano* 6:10950–10964. <https://doi.org/10.1021/nm304505s>.
  36. Peters BM, Noverr MC. 2013. *Candida albicans*-*Staphylococcus aureus* polymicrobial peritonitis modulates host innate immunity. *Infect Immun* 81:2178–2189. <https://doi.org/10.1128/IAI.00265-13>.
  37. Schlecht LM, Peters BM, Krom BP, Freiberg JA, Hansch GM, Filler SG, Jabra-Rizk MA, Shirliff ME. 2015. Systemic *Staphylococcus aureus* infection mediated by *Candida albicans* hyphal invasion of mucosal tissue. *Microbiology* 161:168–181. <https://doi.org/10.1099/mic.0.083485-0>.
  38. Gresham HD, Lowrance JH, Caver TE, Wilson BS, Cheung AL, Lindberg FP. 2000. Survival of *Staphylococcus aureus* inside neutrophils contributes to infection. *J Immunol* 164:3713–3722. <https://doi.org/10.4049/jimmunol.164.7.3713>.
  39. Tuchscherer L, Medina E, Hussain M, Volker W, Heitmann V, Niemann S, Holzinger D, Roth J, Proctor RA, Becker K, Peters G, Loffler B. 2011. *Staphylococcus aureus* phenotype switching: an effective bacterial strategy to escape host immune response and establish a chronic infection. *EMBO Mol Med* 3:129–141. <https://doi.org/10.1002/emmm.201000115>.
  40. Surewaard BG, Deniset JF, Zemp FJ, Amrein M, Otto M, Conly J, Omri A, Yates RM, Kubers P. 2016. Identification and treatment of the *Staphylococcus aureus* reservoir in vivo. *J Exp Med* 213:1141–1151. <https://doi.org/10.1084/jem.20160334>.
  41. Lorenz MC, Bender JA, Fink GR. 2004. Transcriptional response of *Candida albicans* upon internalization by macrophages. *Eukaryot Cell* 3:1076–1087. <https://doi.org/10.1128/EC.3.5.1076-1087.2004>.
  42. Vylkova S, Lorenz MC. 2014. Modulation of phagosomal pH by *Candida albicans* promotes hyphal morphogenesis and requires Stp2p, a regulator of amino acid transport. *PLoS Pathog* 10:e1003995. <https://doi.org/10.1371/journal.ppat.1003995>.
  43. Ballou ER, Avelar GM, Childers DS, Mackie J, Bain JM, Wagener J, Kastora SL, Panea MD, Hardison SE, Walker LA, Erwig LP, Munro CA, Gow NA, Brown GD, MacCallum DM, Brown AJ. 2016. Lactate signalling regulates fungal beta-glucan masking and immune evasion. *Nat Microbiol* 2:16238. <https://doi.org/10.1038/nmicrobiol.2016.238>.
  44. Ovchinnikova ES, Krom BP, Busscher HJ, van der Mei HC. 2012. Evaluation of adhesion forces of *Staphylococcus aureus* along the length of *Candida albicans* hyphae. *BMC Microbiol* 12:281. <https://doi.org/10.1186/1471-2180-12-281>.
  45. Ovchinnikova ES, van der Mei HC, Krom BP, Busscher HJ. 2013. Exchange of adsorbed serum proteins during adhesion of *Staphylococcus aureus* to an abiotic surface and *Candida albicans* hyphae—an AFM study. *Colloids Surf B Biointerfaces* 110:45–50. <https://doi.org/10.1016/j.colsurfb.2013.04.015>.
  46. Harriott MM, Noverr MC. 2010. Ability of *Candida albicans* mutants to induce *Staphylococcus aureus* vancomycin resistance during polymicrobial biofilm formation. *Antimicrob Agents Chemother* 54:3746–3755. <https://doi.org/10.1128/AAC.00573-10>.
  47. Collette JR, Zhou H, Lorenz MC. 2014. *Candida albicans* suppresses nitric oxide generation from macrophages via a secreted molecule. *PLoS One* 9:e96203. <https://doi.org/10.1371/journal.pone.0096203>.
  48. Vylkova S, Lorenz MC. 2017. Phagosomal neutralization by the fungal pathogen *Candida albicans* induces macrophage pyroptosis. *Infect Immun* 85:e00832-16. <https://doi.org/10.1128/IAI.00832-16>.
  49. Segal AW. 2008. The function of the NADPH oxidase of phagocytes and its relationship to other NOXs in plants, invertebrates, and mammals. *Int J Biochem Cell Biol* 40:604–618. <https://doi.org/10.1016/j.biocel.2007.10.003>.
  50. Sibille Y, Reynolds HY. 1990. Macrophages and polymorphonuclear neutrophils in lung defense and injury. *Am Rev Respir Dis* 141:471–501. <https://doi.org/10.1164/ajrccm/141.2.471>.
  51. Gross NT, Chinchilla M, Camner P, Jarstrand C. 1996. Anticryptococcal activity by alveolar macrophages from rats treated with cortisone acetate during different periods of time. *Mycopathologia* 136:1–8. <https://doi.org/10.1007/BF00436653>.
  52. Brattsand R, Linden M. 1996. Cytokine modulation by glucocorticoids: mechanisms and actions in cellular studies. *Aliment Pharmacol Ther* 10(Suppl 2):81–90. <https://doi.org/10.1046/j.1365-2036.1996.22164025.x>.
  53. Flannagan RS, Heit B, Heinrichs DE. 2015. Antimicrobial mechanisms of macrophages and the immune evasion strategies of *Staphylococcus aureus*. *Pathogens* 4:826–868. <https://doi.org/10.3390/pathogens4040826>.
  54. van Kessel KP, Bestebroer J, van Strijp JA. 2014. Neutrophil-mediated phagocytosis of *Staphylococcus aureus*. *Front Immunol* 5:467. <https://doi.org/10.3389/fimmu.2014.00467>.
  55. Guidi-Rontani C. 2002. The alveolar macrophage: the Trojan horse of *Bacillus anthracis*. *Trends Microbiol* 10:405–409. [https://doi.org/10.1016/S0966-842X\(02\)02422-8](https://doi.org/10.1016/S0966-842X(02)02422-8).
  56. Peters BM, Jabra-Rizk MA, O'May GA, Costerton JW, Shirliff ME. 2012. Polymicrobial interactions: impact on pathogenesis and human disease. *Clin Microbiol Rev* 25:193–213. <https://doi.org/10.1128/CMR.00013-11>.
  57. Harriott MM, Noverr MC. 2009. *Candida albicans* and *Staphylococcus aureus* form polymicrobial biofilms: effects on antimicrobial resistance. *Antimicrob Agents Chemother* 53:3914–3922. <https://doi.org/10.1128/AAC.00657-09>.
  58. Diep BA, Otto M. 2008. The role of virulence determinants in community-associated MRSA pathogenesis. *Trends Microbiol* 16:361–369. <https://doi.org/10.1016/j.tim.2008.05.002>.
  59. Freeman SA, Grinstead S. 2014. Phagocytosis: receptors, signal integration, and the cytoskeleton. *Immunol Rev* 262:193–215. <https://doi.org/10.1111/imr.12212>.
  60. Dieu-Nosjean MC, Massacrier C, Homey B, Vanbervliet B, Pin JJ, Vicari A, Lebecque S, Dezutter-Dambuyant C, Schmitt D, Zlotnik A, Caux C. 2000. Macrophage inflammatory protein 3alpha is expressed at inflamed epithelial surfaces and is the most potent chemokine known in attracting Langerhans cell precursors. *J Exp Med* 192:705–718. <https://doi.org/10.1084/jem.192.5.705>.
  61. Feng Z, Jiang B, Chandra J, Ghannoum M, Nelson S, Weinberg A. 2005. Human beta-defensins: differential activity against candidal species and regulation by *Candida albicans*. *J Dent Res* 84:445–450. <https://doi.org/10.1177/154405910508400509>.
  62. Thorley AJ, Goldstraw P, Young A, Tetley TD. 2005. Primary human alveolar type II epithelial cell CCL20 (macrophage inflammatory protein-3alpha)-induced dendritic cell migration. *Am J Respir Cell Mol Biol* 32:262–267. <https://doi.org/10.1165/rcmb.2004-0196OC>.

63. Sierra F, Dubois B, Coste A, Kaiserlian D, Kraehenbuhl JP, Sirard JC. 2001. Flagellin stimulation of intestinal epithelial cells triggers CCL20-mediated migration of dendritic cells. *Proc Natl Acad Sci U S A* 98:13722–13727. <https://doi.org/10.1073/pnas.241308598>.
64. Brown GD, Taylor PR, Reid DM, Willment JA, Williams DL, Martinez-Pomares L, Wong SY, Gordon S. 2002. Dectin-1 is a major beta-glucan receptor on macrophages. *J Exp Med* 196:407–412. <https://doi.org/10.1084/jem.20020470>.
65. Taylor PR, Brown GD, Reid DM, Willment JA, Martinez-Pomares L, Gordon S, Wong SY. 2002. The beta-glucan receptor, dectin-1, is predominantly expressed on the surface of cells of the monocyte/macrophage and neutrophil lineages. *J Immunol* 169:3876–3882. <https://doi.org/10.4049/jimmunol.169.7.3876>.
66. Pietrella D, Bistoni G, Corbucci C, Perito S, Vecchiarelli A. 2006. *Candida albicans* mannoprotein influences the biological function of dendritic cells. *Cell Microbiol* 8:602–612. <https://doi.org/10.1111/j.1462-5822.2005.00651.x>.
67. Netea MG, Marodi L. 2010. Innate immune mechanisms for recognition and uptake of *Candida* species. *Trends Immunol* 31:346–353. <https://doi.org/10.1016/j.it.2010.06.007>.
68. Pérez-Flores G, Hernández-Silva C, Gutiérrez-Escobedo G, De Las Peñas A, Castaño I, Arreola J, Pérez-Cornejo P. 2016. P2X7 from J774 murine macrophages acts as a scavenger receptor for bacteria but not yeast. *Biochem Biophys Res Commun* 481:19–24. <https://doi.org/10.1016/j.bbrc.2016.11.027>.
69. Burnstock G. 2016. P2X ion channel receptors and inflammation. *Purinergic Signal* 12:59–67. <https://doi.org/10.1007/s11302-015-9493-0>.
70. Fairbairn IP, Stober CB, Kumararatne DS, Lammas DA. 2001. ATP-mediated killing of intracellular mycobacteria by macrophages is a P2X(7)-dependent process inducing bacterial death by phagosome-lysosome fusion. *J Immunol* 167:3300–3307. <https://doi.org/10.4049/jimmunol.167.6.3300>.
71. Miller CM, Boulter NR, Fuller SJ, Zakrzewski AM, Lees MP, Saunders BM, Wiley JS, Smith NC. 2011. The role of the P2X(7) receptor in infectious diseases. *PLoS Pathog* 7:e1002212. <https://doi.org/10.1371/journal.ppat.1002212>.
72. Nakano K, Nemoto H, Nomura R, Inaba H, Yoshioka H, Taniguchi K, Amano A, Ooshima T. 2009. Detection of oral bacteria in cardiovascular specimens. *Oral Microbiol Immunol* 24:64–68. <https://doi.org/10.1111/j.1399-302X.2008.00479.x>.
73. Kechschull M, Demmer RT, Papapanou PN. 2010. “Gum bug, leave my heart alone!”—epidemiologic and mechanistic evidence linking periodontal infections and atherosclerosis. *J Dent Res* 89:879–902. <https://doi.org/10.1177/0022034510375281>.
74. Haraszthy VI, Zambon JJ, Trevisan M, Zeid M, Genco RJ. 2000. Identification of periodontal pathogens in atheromatous plaques. *J Periodontol* 71:1554–1560. <https://doi.org/10.1902/jop.2000.71.10.1554>.
75. Kozarov E, Sweier D, Shelburne C, Progulske-Fox A, Lopatin D. 2006. Detection of bacterial DNA in atheromatous plaques by quantitative PCR. *Microbes Infect* 8:687–693. <https://doi.org/10.1016/j.micinf.2005.09.004>.
76. Kozarov EV, Dorn BR, Shelburne CE, Dunn WA, Jr, Progulske-Fox A. 2005. Human atherosclerotic plaque contains viable invasive *Actinobacillus actinomycetemcomitans* and *Porphyromonas gingivalis*. *Arterioscler Thromb Vasc Biol* 25:e17–e18. <https://doi.org/10.1161/01.ATV.0000155018.67835.1a>.
77. Nakano K, Wada K, Nomura R, Nemoto H, Inaba H, Kojima A, Naka S, Hokamura K, Mukai T, Nakajima A, Umemura K, Kamisaki Y, Yoshioka H, Taniguchi K, Amano A, Ooshima T. 2011. Characterization of aortic aneurysms in cardiovascular disease patients harboring *Porphyromonas gingivalis*. *Oral Dis* 17:370–378. <https://doi.org/10.1111/j.1601-0825.2010.01759.x>.
78. Gaetti-Jardim E, Jr, Marcelino SL, Feitosa AC, Romito GA, Avila-Campos MJ. 2009. Quantitative detection of periodontopathic bacteria in atherosclerotic plaques from coronary arteries. *J Med Microbiol* 58:1568–1575. <https://doi.org/10.1099/jmm.0.013383-0>.
79. Gillum AM, Tsay EY, Kirsch DR. 1984. Isolation of the *Candida albicans* gene for orotidine-5'-phosphate decarboxylase by complementation of *S. cerevisiae* ura3 and *E. coli* pyrF mutations. *Mol Gen Genet* 198:179–182. <https://doi.org/10.1007/BF00328721>.
80. Kennedy AD, Porcella SF, Martens C, Whitney AR, Braughton KR, Chen L, Craig CT, Tenover FC, Kreiswirth BN, Musser JM, DeLeo FR. 2010. Complete nucleotide sequence analysis of plasmids in strains of *Staphylococcus aureus* clone USA300 reveals a high level of identity among isolates with closely related core genome sequences. *J Clin Microbiol* 48:4504–4511. <https://doi.org/10.1128/JCM.01050-10>.
81. Li J, Busscher HJ, van der Mei HC, Norde W, Krom BP, Sjollem J. 2011. Analysis of the contribution of sedimentation to bacterial mass transport in a parallel plate flow chamber: part II: use of fluorescence imaging. *Colloids Surf B Biointerfaces* 87:427–432. <https://doi.org/10.1016/j.colsurfb.2011.06.002>.